nature climate change

LETTERS

PUBLISHED ONLINE: 29 JULY 2012 | DOI: 10.1038/NCLIMATE1631

Enhanced poleward moisture transport and amplified northern high-latitude wetting trend

Xiangdong Zhang[1]*, Juanxiong He[1,2], Jing Zhang[3], Igor Polyakov[1], Rüdiger Gerdes[4], Jun Inoue[5] and Peili Wu[6]

Observations and climate change projections forced by greenhouse gas emissions have indicated a wetting trend in northern high latitudes, evidenced by increasing Eurasian Arctic river discharges[1–3]. The increase in river discharge has accelerated in the latest decade and an unprecedented, record high discharge occurred in 2007 along with an extreme loss of Arctic summer sea-ice cover[4–6]. Studies have ascribed this increasing discharge to various factors attributable to local global warming effects, including intensifying precipitation minus evaporation, thawing permafrost, increasing greenness and reduced plant transpiration[7–11]. However, no agreement has been reached and causal physical processes remain unclear. Here we show that enhancement of poleward atmospheric moisture transport (AMT) decisively contributes to increased Eurasian Arctic river discharges. Net AMT into the Eurasian Arctic river basins captures 98% of the gauged climatological river discharges. The trend of 2.6% net AMT increase per decade accounts well for the 1.8% per decade increase in gauged discharges and also suggests an increase in underlying soil moisture. A radical shift of the atmospheric circulation pattern induced an unusually large AMT and warm surface in 2006–2007 over Eurasia, resulting in the record high discharge.

Theoretical estimates by the Clausius–Clapeyron equation and observations have indicated an increase of ~7% K^{-1} in lower tropospheric moisture content under global warming forcing[12,13]. As a consequence, poleward AMT is expected to be enhanced, even if changes in atmospheric circulation are trivial[13]. Accordingly, precipitation would increase, contributing to an intensified hydrological cycle, especially in northern high latitudes. This has been manifested in Eurasian Arctic rivers[1,14]. Meanwhile, modelling studies suggest that global-warming-induced degradation of permafrost, increase in greenness and reduction of plant transpiration in northern high latitudes may also contribute to the intensified hydrological cycle and increased river discharges[8–11].

However, large uncertainties exist in observations and models owing to the lack of direct or accurate measurement and realistic treatment of the above-mentioned processes[15–17]. For example, precipitation measurements are sparse in northern high latitudes and exhibit large cold-season biases ranging from 50 to 100% (refs 14,18); state-of-the-art climate models have simulated and projected substantially different rates of increasing precipitation[3]. On the other hand, northern high-latitude atmospheric circulation has experienced amplified temporal fluctuations and radical spatial shifts[5,19], which would further strengthen AMT and alter AMT pathways under increasing atmospheric moisture. This dynamic effect has not been well resolved or has been neglected in many studies. It therefore remains unclear which physical process is the leading driver of the observed increase in Eurasian river discharges, including the record high 2007 discharge[6].

To better understand the predominant driver behind the increased river discharges, we examined AMT. The net AMT for a closed river basin represents regionally integrated precipitation minus evapotranspiration and the changing rate of atmospheric water content. River discharge represents a spatial integral of net surface water budget in the river catchment, including water input from precipitation and loss by evapotranspiration, subject to modification by soil and vegetation water storage. As mentioned above, large errors and sparse observations exist in precipitation measurements. Evapotranspiration acquires even larger uncertainties owing to empirical assumptions in its calculation. Nevertheless, wind and specific humidity used in AMT computation are regularly measured at meteorological stations with great fidelity. The use of AMT, therefore, should enable surface water budgets to be quantified with enhanced accuracy, improving understanding of the impacts of atmospheric circulation dynamics on the intensifying hydrological cycle.

The data used include wind and specific humidity from the National Centers for Environmental Prediction–National Center for Atmospheric Research (NCEP–NCAR) reanalysis[20], with mass-correction by an improved approach that builds on a previously suggested methodology[21] (Supplementary Information). The gauged monthly river discharges are from the Arctic Rapid Integrated Monitoring System (http://rims.unh.edu). The Ob, Yenisei and Lena are the largest Eurasian Arctic rivers, and the longest and most complete observations, back to the 1930s, have been made at their most downstream gauge stations (Supplementary Information). During our analysis period of 1948–2008, the gauged discharges from these three rivers amounted to 1,579 $km^3\ yr^{-1}$ in climatology, representing an area of $795 \times 10^4\ km^2$ (Fig. 1), 66.4% of the total gauged climatological Eurasian Arctic river discharges of 2,379 $km^3\ yr^{-1}$ and 60.3% of the total gauged Eurasian river catchment area of $1{,}318 \times 10^4\ km^2$. We therefore chose these three river basins as representative of all Eurasian Arctic rivers to study their changes.

To lay solid groundwork for bridging AMT and river discharges, we conducted a climatological analysis by computing annual net vertically integrated AMT (equation (1)) within the

[1]International Arctic Research Center and Department of Atmospheric Sciences, University of Alaska Fairbanks, 930 Koyukuk Dr., Fairbanks, Alaska 99775, USA, [2]Institute of Atmospheric Physics, Chinese Academy of Sciences, Beijing 100029, China, [3]Department of Physics and Energy and Environmental Systems, North Carolina A&T State University, Greensboro, North Carolina 27411, USA, [4]Alfred Wegener Institute for Polar and Marine Research, Bussestrasse 24, Bremerhaven D-27570, Germany, [5]Research Institute for Global Change, Japan Agency for Marine-Earth Science and Technology, 2-15 Natsushima-cho, Yokosuka, Kanagawa 237-0061, Japan, [6]Met Office Hadley Centre, FitzRoy Road, Exeter EX1 3PB, UK. *e-mail: xdz@iarc.uaf.edu.

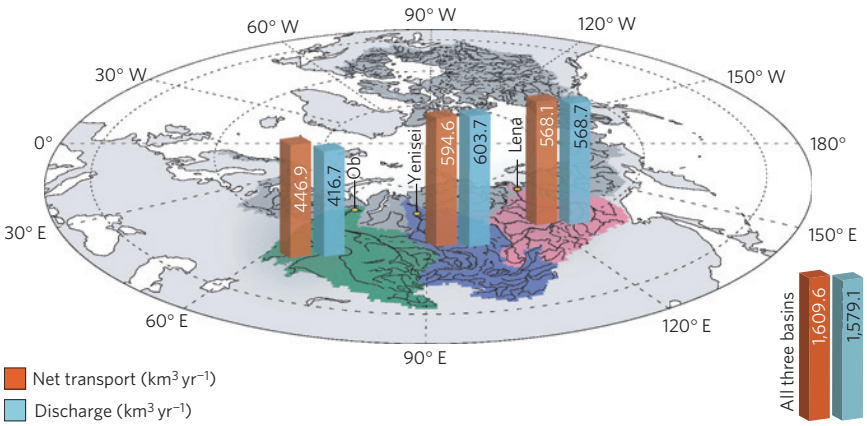

Figure 1 | Climatological annual net AMT and river discharges. Climatology of annual net AMT converged into and river discharges from the three large Eurasian rivers, Ob, Yenisei and Lena, from 1948 to 2008. Red and sky blue columns, as well as their embedded values, show annual net AMT and river discharge, respectively. Yellow dots denote the location of the most downstream gauge stations where the river discharges were observed. Shaded dark grey and coloured areas demonstrate the Arctic river drainage basins; black lines within show streams and rivers. Green, blue and magenta highlight the Ob, Yenisei and Lena river basins, respectively.

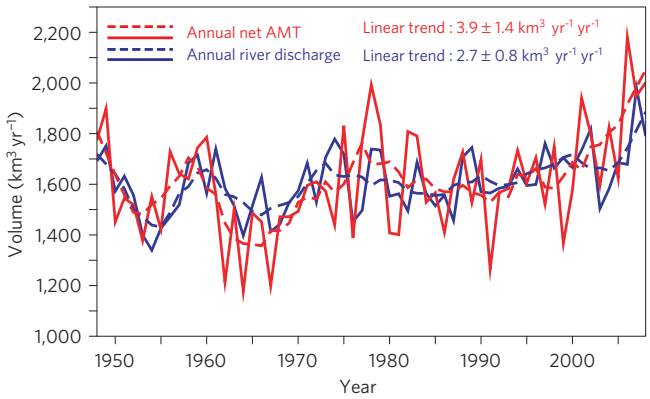

Figure 2 | Year-by-year annual net AMT and river discharge. Annual net AMT converged into the Ob, Yenisei and Lena river basins (red solid line) and annual discharge from these three rivers (blue solid line) from 1948 to 2008. The five-year running means were applied to detect QDV of net AMT (red dashed line) and discharge (blue dashed line). The linear trends are derived from the linear regression.

three representative river basins from 1948 to 2008 (Fig. 1). The climatological annual net AMT into the river basins is quantified as 1,610 $km^3\ yr^{-1}$ including 447 $km^3\ yr^{-1}$, 595 $km^3\ yr^{-1}$ and 568 $km^3\ yr^{-1}$ into the Ob, Yenisei and Lena basins, respectively. Comparison with river discharges indicates that annual net AMT accurately captures the gauged climatological discharges, not only for all basins but also for each individual basin with differences below 2%, except for the Ob River with 7.2%, perhaps owing to its significant endorheic component. This provides strong evidence that AMT has been the fundamental contributor to climatological river discharges during the past 60 years.

Superimposed on their climatologies, the annual net AMT and river discharges exhibit large interannual–decadal variability and conspicuous long-term changes (Fig. 2). When tracking year-by-year fluctuations, we readily find that discharge is generally consistent with net AMT in both phase and amplitude; AMT takes a lead in many years owing to its different seasonality from discharge (Supplementary Fig. S3). Most discharge occurs between mid-May and October; peak volume appears near the beginning of this timeframe. Much of this discharge comes from AMT that was stored as snow until the spring and then discharged into the river basins. Considering the different seasonality, we conducted a statistical analysis based on water year (September–August, Supplementary Fig. S4), showing a detrended correlation coefficient of 0.46 between discharge and net AMT interannual variability at a 99.8% level of significance by using the non-parametric random phase method[22]. This suggests that the annual net AMT variability explains a predominant fraction of the discharge variability, indicating the former's leading role in regulating the latter. The remaining variance of variability could be attributable to year-to-year alteration of land-surface properties, such as permafrost, vegetation, groundwater storage and so on.

Annual net AMT and discharges also show quasi-decadal scale variability (QDV, Fig. 2). The QDV has an obviously shorter time period than the previously detected multidecadal variability of Arctic surface air temperature[23,24] (SAT), excluding a sole driving role of multidecadal SAT variability in AMT and river discharge QDV. This mismatch suggests dynamic and thermodynamic interplays within AMT. Atmospheric capacity for holding water fluctuates with SAT multidecadal variability. Nevertheless, the actual regional atmospheric water budgets are critically determined by dynamic processes of atmospheric circulation. The mismatch may also result from low-latitude variability but needs to be examined in further study. The QDV component of net AMT and discharges peaked around the 1950s, 1970s and 2000s. The detrended correlation coefficient between the net AMT and discharge QDV components reaches 0.72, indicating an increased governing role of AMT in river discharge on quasi-decadal scales. Interestingly, the positive QDV phase lasted for a longer time in the latest decade than previously, perhaps implying a tendency of frequency reddening shift.

The long-term upward trends of the annual net AMT and river discharges are conspicuous from 1948 to 2008. Discharges increased at a rate of $2.7 \pm 0.8\ km^3\ yr^{-1}\ yr^{-1}$. A previous study identified a trend of discharge increase at $2.0 \pm 0.7\ km^3\ yr^{-1}\ yr^{-1}$ for 1936–1999 from six Eurasian rivers[1]. We calculated this trend focusing only on our selected three largest rivers and found an increase of $1.7 \pm 0.7\ km^3\ yr^{-1}\ yr^{-1}$ from 1936 to 1999. Our newly estimated trend of $2.7 \pm 0.8\ km^3\ yr^{-1}\ yr^{-1}$ from 1948 to 2008, therefore, suggests an accelerated discharge increase when the timeframe shifts to the latest decades. The increasing rate is enhanced by 59%. Specifically, the previously estimated total discharge from six Eurasian rivers increased by 7% from 1936 to 1999, suggesting that the trend-based annual discharge in the late 1990s was about 128 $km^3\ yr^{-1}$ greater than in the mid-1930s. Our result here reveals that the discharge increase from the selected three rivers was

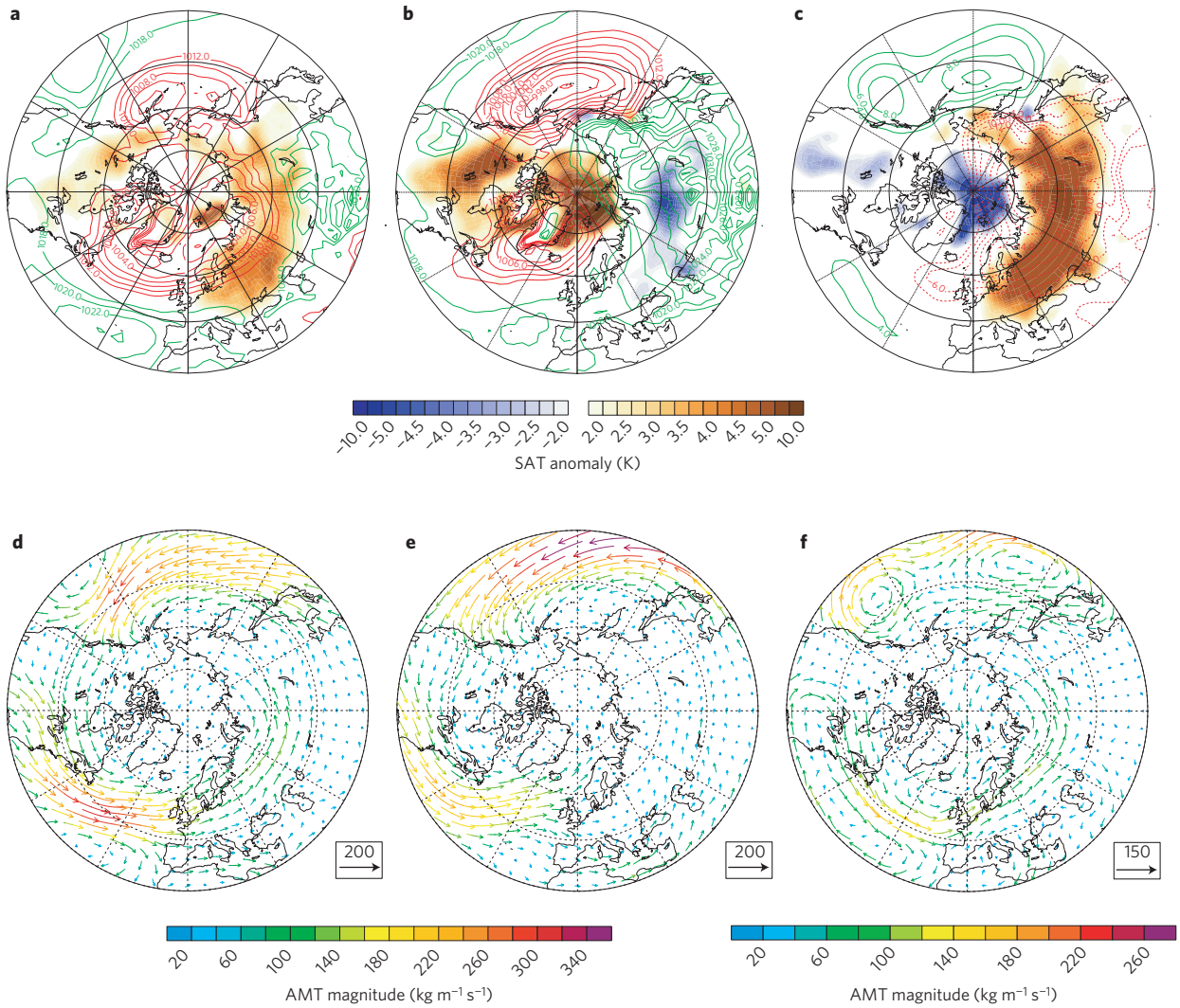

Figure 3 | ARP-based composite analysis of sea-level pressure, SAT and AMT. The sea-level pressure (red and green lines) and SAT anomalies (shaded in colours) in the **a**, positive and **b**, negative ARP phases. **c** Their differences are depicted. The AMT in the **d**, positive and **e**, negative ARP phases and **f**, their differences. The SAT anomalies were computed using a climatology derived from 1958 to 1997. The colours in **d**–**f** show the AMT magnitudes.

further amplified to 10.6% (1.8% per decade) based on the linear trend from 1948 to 2008. The discharge from these three rivers is 161 $km^3\ yr^{-1}$ higher than that in the late 1940s.

Net AMT increased even more than the river discharges, at a rate of $3.9 \pm 1.4\ km^3\ yr^{-1}\ yr^{-1}$ from 1948 to 2008; a net 232 $km^3\ yr^{-1}$ more atmospheric water was transported into the three river basins in the 2000s than in the late 1940s. This amount indicates a 15.6% increase (2.6% per decade) in net AMT during the past 60 years, sufficient to supply the increase of 10.6% in river discharges discussed above. Considering that the water supply from the atmosphere is the predominant source of surface water, and the net AMT and river discharge computed above are climatologically close, our results suggest that the increase in AMT, rather than local water recycling owing to changes in land-surface properties, is a leading driver of the increased river discharges.

Furthermore, the net AMT increased more than the river discharge, suggesting increased soil moisture, depending on the amount of water remaining in the atmosphere. To clarify this, we computed atmospheric water content over the three river basins for 1960–1969 and 1999–2008 when net AMT and river discharge went to minimum and maximum, respectively (Fig. 2). The annual mean water content was about 93.6 (97.0) km^3 during 1960–1969 (1999–2008), indicating an increase of 3.4 km^3 (~3.6%). Similar analysis shows that the annual mean net AMT increased about 355 km^3 (~24.8%), from 1,431 to 1,786 km^3, and the annual mean river discharge increased about 182 km^3 (~11.8%), from 1,533 to 1,714 km^3, between these two periods. Consequently, most of the increased water from AMT went through the atmosphere into the underlying soil and rivers. Given that net AMT represents regionally integrated precipitation minus evapotranspiration, precipitation dominates evapotranspiration, which may lead to wetter soil on an annual basis and perhaps provide a physical interpretation of the increased groundwater storage measured by the Gravity Recovery and Climate Experiment satellites[25].

Net AMT also demonstrated larger-amplitude interannual and decadal fluctuations than did river discharges (Fig. 2). This could be accounted for by the longer memory of land-surface processes than of atmosphere and the slowly varying modulation of water storage in soil and vegetation, both of which can damp amplitude of discharge fluctuations. Moreover, the warming climate has resulted in thawing permafrost, which may increase infiltration of soil water, thereby reducing surface runoff and probably increasing baseflow generation. The enlarged phase lag between the net AMT and discharge in recent years could be a manifestation of the change in land surface. However, these finer-scale processes have not been quantitatively explained; this requires further investigation.

A record high discharge was reported in 2007 (refs 6,26), accompanying extreme loss of summer sea-ice cover[4,5]. A closer examination reveals that net AMT had reached a record high earlier, in 2006, and continued to be high in 2007 (Fig. 2). We identified that the occurrence of extreme AMT and discharge events can be attributed to the same causal factor responsible for the rapid sea-ice changes, that is, the radical shift of the atmospheric circulation with positive polarization of the Arctic rapid-change pattern (ARP) in 2006–2007, as a consequence of an accelerated northeastward shift of North Atlantic storm tracks[5,27]. Composite analysis based on the ARP index indicates an intensified Icelandic low that extended far northeastwards into the Barents Sea and towards the Eurasian coast when positive ARP dominated during 2006–2007, compared with the extent when negative ARP dominated before 2006 (Fig. 3 and Supplementary Information). Meanwhile, the Siberian high substantially weakened and contracted southwards as ARP transitioned from negative to positive.

Corresponding to the atmospheric circulation changes, large warm SAT anomalies occurred over the Eurasian continent owing to enhanced heat transport by the intensified Icelandic low during 2006–2007 when ARP swiftly went to positive phase (Fig. 3). The simultaneously weakened Siberian high also contributed to the warm anomalies by reducing outgoing radiative cooling. Simultaneously, AMT, calculated by equation (2), was obviously intensified over the North Atlantic and pronouncedly extended into the Eurasian river basins. By contrast, AMT weakened and curved strongly northeastwards over the North Atlantic before it reached the Eurasian continent before 2006 when ARP was negative. As a result, an unusually large net AMT occurred over the Eurasian river basins. The interplay of large AMT and warmed SAT led to record high river discharges.

Here we quantitatively establish the relationship between dynamic AMT and Eurasian river discharges in a warming climate (Supplementary Table S1). Although increased global atmospheric water content is attributed to rising air temperature, a changed atmospheric circulation is the route by which global warming forcing exerts dynamic effects on water redistribution. The increased river discharge and precipitation over Eurasian river basins mainly originated from outside through enhanced AMT, rather than through local water recycling. Before the 2007 record high discharge, an unprecedentedly high AMT and anomalously large warm SAT occurred. Their phase difference reinforces our earlier finding that changes in atmospheric circulation lead the observed rapid changes in many other components of the Arctic climate system, exemplified by the record low sea ice and record high river discharge in 2007 (refs 4–6). This also clarifies that the record high river discharge cannot be attributed to a hypothesized enhancement of evaporation owing to extremely reduced sea-ice cover (Supplementary Information). Our results here have great potential to improve understanding of hydrological interactions among climate system components, such as water vapour's contribution to polar amplification, and carry important implications for density-driven ocean circulation in the Arctic and North Atlantic that impact sea-ice mass balance, broad-scale climate variability and ecosystems.

Methods

AMT and net AMT converged into the river basin. To compute AMT and its net convergence into the river basin, we used original six-hourly spectral output in the terrain-following σ coordinate from the NCEP–NCAR reanalysis, instead of the post-processed physical variables in spherical and pressure (p) coordinates[20]. The σ coordinate is a scaled p coordinate by surface pressure, that is, $\sigma = p/p_s$. The NCEP–NCAR reanalysis has a horizontal spatial resolution of T62 ($\sim$1.875° in spherical coordinate) with 28σ levels vertically. Using the model assimilation system's original σ coordinate data avoids boundary problems caused by the intercept between pressure surface and terrain in the regular p coordinate and errors resulting from interpolation from the model's σ levels to p levels. σ-level data also better represent boundary-layer structures, where humidity usually reaches maximum. The net AMT converged into the river basin in the σ coordinate is expressed by:

$$\text{Net AMT} = \int_{\text{basin}} \left(\nabla \cdot \int_1^0 \frac{p_s q \mathbf{v}}{g} \, \mathrm{d}\sigma \right) \mathrm{d}S \quad (1)$$

and the AMT at each grid point is:

$$\text{AMT} = \frac{1}{g} \int_1^0 p_s q \mathbf{v} \, \mathrm{d}\sigma \quad (2)$$

where p_s is the surface pressure, q the specific humidity, $\mathbf{v}$ the wind vector and g the gravity acceleration. $\int_{\text{basin}} \cdot \mathrm{d}S$ is the areal integral over the river basin. The wind vector $\mathbf{v}$ used here is mass-corrected to insure global dry air mass conservation and data homogeneity throughout the study period (see Supplementary Information).

To accurately compute AMT, we directly used spectral coefficient data output from the model assimilation system available for divergence, vorticity and specific humidity. We applied spectral decomposition to express AMT by using the available spectral coefficients for its quantitative calculation. Details about spectral decomposition can be found in the literature[28]. Finally, we used the first-order conservative remapping approach to interpolate AMT data onto the 0.5° × 0.5° pan-Arctic river drainage data set[29,30].

Received 12 March 2012; accepted 21 June 2012; published online 29 July 2012

References

1. Peterson, B. J. *et al*. Increasing river discharge to the Arctic Ocean. *Science* **298,** 2171–2173 (2002).
2. Wu, P., Wood, R. & Stott, P. Human influence on increasing Arctic river discharges. *Geophys. Res. Lett.* **32,** L02703 (2005).
3. Kattsov, V., Walsh, J. E., Govorkova, V., Pavlova, T. & Zhang, X. Arctic Ocean freshwater budget components in simulations with the IPCC AR4 AOGCMs. *J. Hydrometeorol.* **8,** 571–589 (2007).
4. Comiso, J. C., Parkinson, C. L., Gersten, R. & Stocket, L. Accelerated decline in the Arctic sea ice cover. *Geophys. Res. Lett.* **35,** L01703 (2008).
5. Zhang, X., Sorteberg, A., Zhang, J., Gerdes, R. & Comiso, J. C. Recent radical shifts of atmospheric circulations and rapid changes in Arctic climate system. *Geophys. Res. Lett.* **35,** L22701 (2008).
6. Shiklomanov, A. I. & Lammers, R. B. Record Russian river discharge in 2007 and the limits of analysis. *Environ. Res. Lett.* **4,** 045015 (2009).
7. Zhang, X. *et al*. Detection of human influence on twentieth-century precipitation trends. *Nature* **448,** 461–465 (2007).
8. Oelke, C., Zhang, T. & Serreze, M. C. Modeling evidence for recent warming of the Arctic soil thermal regime. *Geophys. Res. Lett.* **31,** L07208 (2004).
9. Zhang, J. & Walsh, J. E. Thermodynamic and hydrological impacts of increasing greenness in northern high latitudes. *J. Hydrometeorol.* **7,** 1147–1163 (2006).
10. Zhang, J. & Walsh, J. E. Relative impacts of vegetation coverage and leaf area index on climate change in a greener north. *Geophys. Res. Lett.* **34,** L15703 (2007).
11. Betts, R. A. *et al*. Projected increase in continental runoff due to plant responses to increasing carbon dioxide. *Nature* **448,** 1037–1042 (2007).
12. Wentz, F. J. & Schabel, M. Precise climate monitoring using complementary satellite data sets. *Nature* **403,** 414–416 (2000).
13. Held, I. M. & Soden, B. J. Robust responses of the hydrological cycle to global warming. *J. Clim.* **19,** 5686–5699 (2006).
14. Pavelsky, T. M. & Smith, L. C. Intercomparison of four global precipitation data sets and their correlation with increased Eurasian river discharge to the Arctic Ocean. *J. Geophys. Res.* **111,** D21112 (2006).
15. Serreze, M. *et al*. Large-scale hydro-climatology of the terrestrial Arctic drainage system. *J. Geophys. Res.* **108,** 8160 (2003).
16. McClelland, J. W., Holmes, R. M., Peterson, B. J. & Stieglitz, M. Increasing river discharge in the Eurasian Arctic: Consideration of dams, permafrost thaw, and fires as potential agents of change. *J. Geophys. Res.* **109,** D18102 (2004).
17. Dai, A., Qian, T., Trenberth, K. E. & Milliman, J. D. Changes in continental freshwater discharge from 1948 to 2004. *J. Clim.* **22,** 2773–2792 (2009).
18. Yang, D., Kane, D., Zhang, Z., Legates, D. & Goodison, B. Bias corrections of long-term (1973–2004) daily precipitation data over the northern regions. *Geophys. Res. Lett.* **32,** L19501 (2005).
19. Thompson, D. W. J. & Wallace, J. M. The Arctic oscillation signature in the wintertime geopotential height and temperature fields. *Geophys. Res. Lett.* **25,** 1297–1300 (1998).
20. Kistler, R. *et al*. The NCEP–NCAR 50–year reanalysis: Monthly means CD–ROM and documentation. *Bull. Am. Meteorol. Soc.* **82,** 247–268 (2001).
21. Trenberth, K. E. Climate diagnostics from global analyses: Conservation of mass in ECMWF analyses. *J. Clim.* **4,** 707–722 (1991).

22. Ebisuzaki, W. A method to estimate the statistical significance of a correlation when the data are serially correlated. *J. Clim.* **10,** 2417–2153 (1997).
23. Polyakov, I. *et al.* Variability and trends of air temperature and pressure in the maritime Arctic, 1875–2000. *J. Clim.* **16,** 2067–2077 (2003).
24. Overland, J. E., Spillane, M. C., Percival, D. B., Wang, M. & Mofjeld, H. O. Seasonal and regional variation of pan-Arctic surface air temperature over the instrumental record. *J. Clim.* **17,** 3263–3282 (2004).
25. Muskett, R. R. & Romanovsky, V. Groundwater storage changes in arctic permafrost watersheds from GRACE and *in situ* measurements. *Environ. Res. Lett.* **4,** 045009 (2009).
26. Rawlins, M. A., Serreze, M. C., Schroeder, R., Zhang, X. & McDonald, K. C. Diagnosis of the record discharge of Arctic-draining Eurasian rivers in 2007. *Environ. Res. Lett.* **4,** 045011 (2009).
27. Zhang, X., Walsh, J. E., Zhang, J., Bhatt, U. S. & Ikeda, M. Climatology and interannual variability of Arctic cyclone activity, 1948–2002. *J. Clim.* **17,** 2300–2317 (2004).
28. Jarraud, M. & Simmons, A. J. *Proc.1983 ECMWF Seminar on Numerical Methods for Weather Prediction*, Vol. II, 1–60 (Reading, ECMWF, 1983).
29. Jones, P. W. First- and second-order conservative remapping schemes for grids in spherical coordinates. *Mon. Weath. Rev.* **127,** 2204–2210 (1999).
30. Vorosmarty, C. J., Fekete, B. M., Meybeck, M. & Lammers, R. B. Geomorphometric attributes of the global system of rivers at 30-minute spatial resolution. *J. Hydrol.* **237,** 17–39 (2000).

Acknowledgements

We are grateful to J. E. Walsh for comments that have improved the content and presentation of this paper. We also thank C. Stephenson for his assistance in preparing Fig. 1. The NOAA-ESRL Physical Sciences Division made the NCEP–NCAR reanalysis data available online. The Arctic Region Supercomputing Center supplied computational resources. This work was supported by the US National Science Foundation, the Japan Agency for Marine-Earth Science and Technology and the Joint DECC/Defra Met Office Hadley Centre Climate Programme.

Author contributions

X.Z. designed the research, analysed data, wrote the paper and participated in computation and figure plotting. J.H. conducted computation and figure plotting. J.Z. participated in computation and figure plotting. J.H., J.Z., I.P., R.G., J.I. and P.W. contributed to data analysis and paper writing.

Additional information

Supplementary information is available in the online version of the paper. Reprints and permissions information is available online at www.nature.com/reprints. Correspondence and requests for materials should be addressed to X.Z.

Competing financial interests

The authors declare no competing financial interests.